Surface electronic structure of Pb/Cu(100): surface band filling and folding

2009 J. Phys.: Condens. Matter 21 474216

(http://iopscience.iop.org/0953-8984/21/47/474216)

J. Phys.: Condens. Matter **21** (2009) 474216 (12pp) doi:10.1088/0953-8984/21/47/474216

Surface electronic structure of Pb/Cu(100): surface band filling and folding

V Joco[1], J Martínez-Blanco[1], P Segovia[1], I Vobornik[2] and E G Michel[1]

[1] Departamento de Física de la Materia Condensada, Universidad Autónoma de Madrid, 28049 Madrid, Spain
[2] TASC National Laboratory, INFM-CNR, SS 14, km 163.5, I-34149, Trieste, Italy

Received 14 April 2009
Published 5 November 2009
Online at stacks.iop.org/JPhysCM/21/474216

Abstract
We report an investigation into the surface electronic structure of Pb/Cu(100) in the submonolayer coverage range. A prominent surface band is detected in the whole coverage range analysed. The band is gradually filled as Pb coverage increases. For a Pb coverage of 0.375 ML, corresponding to the c(4 × 4) phase, a strong c(4 × 4) folding of this state is observed in the valence band. The origin of these results and the nature of the surface electronic structure of Pb/Cu(100)-c(4 × 4) are discussed.

(Some figures in this article are in colour only in the electronic version)

1. Introduction

Due to its simplicity, the physics of low-dimensional systems provides a fundamental understanding of complex processes related to the electronic structure. Surface reconstructions and phase transitions are an example of this [1–3]. The particular case when a gain in electronic energy is important has deserved attention in recent years due to its implications in the physics of complex materials [4–7]. An important example of this kind is the formation of a charge density wave, a macroscopically coherent state with very interesting properties [8]. The particular case of submonolayer amounts of Pb grown on Cu(100) has received ample attention in the past [9–20], due to both its basic interest and the applications of Pb atoms as surfactants for epitaxial growth. We summarize in the following a few important properties of this system relevant for the results of this paper. For a more detailed account we refer the reader to [19, 20].

Pb on Cu(100) is a lattice-mismatched system exhibiting a rich and complex phenomenology. On the one hand, Pb and Cu do not mix in the bulk, but Pb atoms intermix with Cu for very low coverages [16] and at least the c(4 × 4) phase, observed in the submonolayer coverage range, can be understood as a surface alloy. Pb atoms, as several other elements of the IIIa, IVa and Va groups, are a surfactant for the epitaxial growth on Cu [15]. Several different surface structures with complex properties and phase transitions are observed in the submonolayer coverage range [9–12]. The growth mode of Pb on Cu(100) is Stranski–Krastanov, so that a dense Pb layer is formed for 0.6 monolayers (MLs) and island growth is observed for higher coverages. There are different surface reconstructions for coverages below 0.6 ML: c(4 × 4) (for 0.375 ML), c(2 × 2) (for 0.5 ML) and c($5\sqrt{2} \times \sqrt{2}$)R45° (for 0.6 ML). The atomic model of these phases is shown in figure 1. The c(4 × 4) structure is a Cu–Pb surface alloy with Cu_4Pb_3 composition [17], while the c(2 × 2) reconstruction is interpreted as a simple arrangement of Pb atoms occupying one half of all available Cu(100) hollow sites [10, 11, 17]. Above 0.5 ML and below 0.6 ML, a c(2 × 2) phase with split superstructure spots is observed. The spot splitting is due to antiphase domain boundaries inserted into the c(2 × 2) structure [10] (see figure 1(c)). For a critical coverage of 0.6 ML, a regular distribution of linear domain boundaries is observed. This domain boundary arrangement is characterized by the regular succession of three rows of Pb atoms occupying the same kind of hollow site (see figure 1(d)). The long-range order of this structure corresponds to a c($5\sqrt{2} \times \sqrt{2}$)R45° conventional unit cell [12–15], and it could be described as a periodic sequence of long-range ordered linear antiphase domain boundaries defining Pb stripes of three atomic rows'

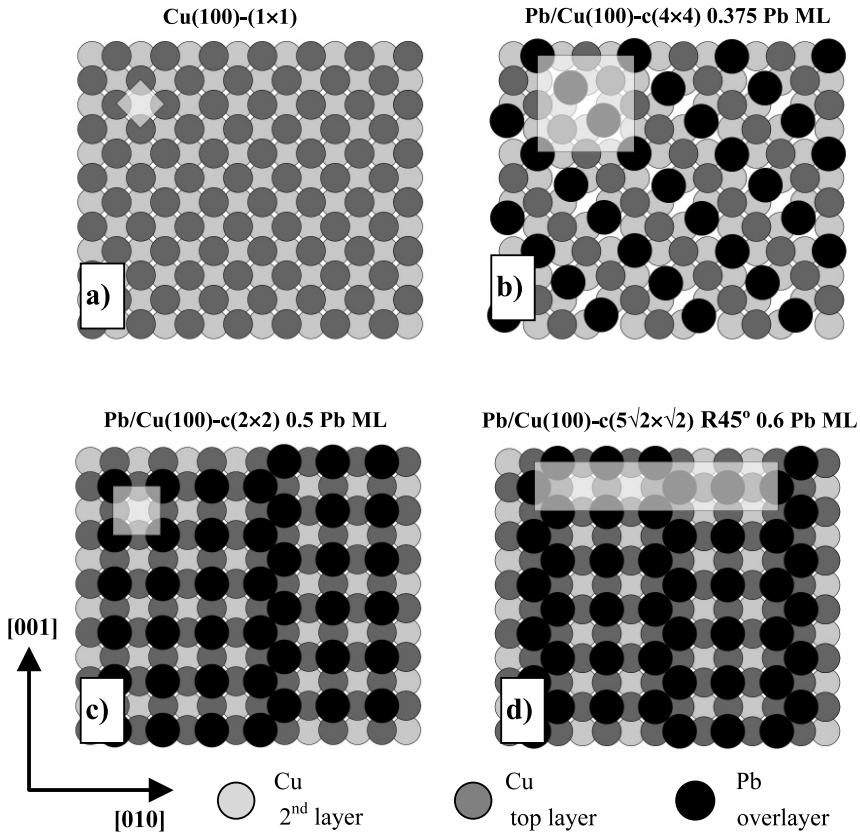

Figure 1. Literature atomic models of unreconstructed Cu(100) surface (a) and main submonolayer phases of Pb/Cu(100) ((b)–(d)). Structure and coverage are shown on top of each model. The unit cell of each structure is drawn as a grey rectangle. (c) shows two antiphase domains and an antiphase domain boundary.

width. The formation of antiphase domain boundaries permits us to accommodate extra Pb atoms with respect to the c(2 × 2) phase. Indeed, the formation of the domain boundaries is a way to compress the c(2 × 2) structure. The crystalline structure of these phases has been established from LEED I/V analysis [10–12]. All the submonolayer phases melt in the 500–570 K range [13–20], a behaviour that has deserved some attention due to the interesting properties of two-dimensional phase transitions [13].

The (100) surfaces of noble metals present frequently reconstructions of the type $(n\sqrt{2} \times m\sqrt{2})$R45° (primitive or centred), specially for adsorbates in the groups IIIa, IVa and Va [25]. Different studies have concluded that Fermi surface nesting and gapping plays an important role in the stabilization of several surface phases of this family. In particular, it has been proposed that In/Cu(100)-$(9\sqrt{2} \times 2\sqrt{2})$R45° [21, 22], In/Cu(100)-$(2\sqrt{2} \times 2\sqrt{2})$R45° [23], and Sn/Cu(100)-p$(3\sqrt{2} \times \sqrt{2})$R45° [24] are stabilized by a gain in electronic energy with respect to a high temperature phase of simpler structure. The $(n\sqrt{2} \times m\sqrt{2})$R45° phases are interpreted as a surface charge density wave [21–24, 28] with novel features (strong coupling, long coherence range) [25].

In this paper we analyse the evolution of the surface electronic structure of Pb/Cu(100) for a Pb coverage range between 0 and 0.6 ML. Special attention has been paid to the surface states observed in the projected band gaps of the Cu(100) surface. During the formation of several phases for increasing Pb coverage, a prominent surface state observed for all submonolayer phases is filled by electrons. The filling of these electronic states takes place gradually and the surface reconstructions put their fingerprint to the electronic structure and vice versa. Due to the rich variety of surface reconstructions, the Pb/Cu(100) system is a good model system for studying the interplay between the surface crystalline and electronic structure. Each main phase described before presents its own electronic structure peculiarities. We analyse in this paper the properties of the c(4 × 4) phase, while the specific features of the c$(5\sqrt{2} \times \sqrt{2})$R45° phase have been described in a previous publication [27].

2. Experiment

Two different ultrahigh vacuum chambers were used to perform angle-resolved photoemission spectroscopy (ARPES) and low-energy electron diffraction (LEED) experiments. The first apparatus received He I radiation from a plasma source (Gammadata) and uses an ARUPS-10 electron analyzer. The energy resolution was set to 80 meV and the angle resolution was 0.5°. The second UHV chamber receives synchrotron light from the Elettra storage ring in Trieste (Italy) and it is

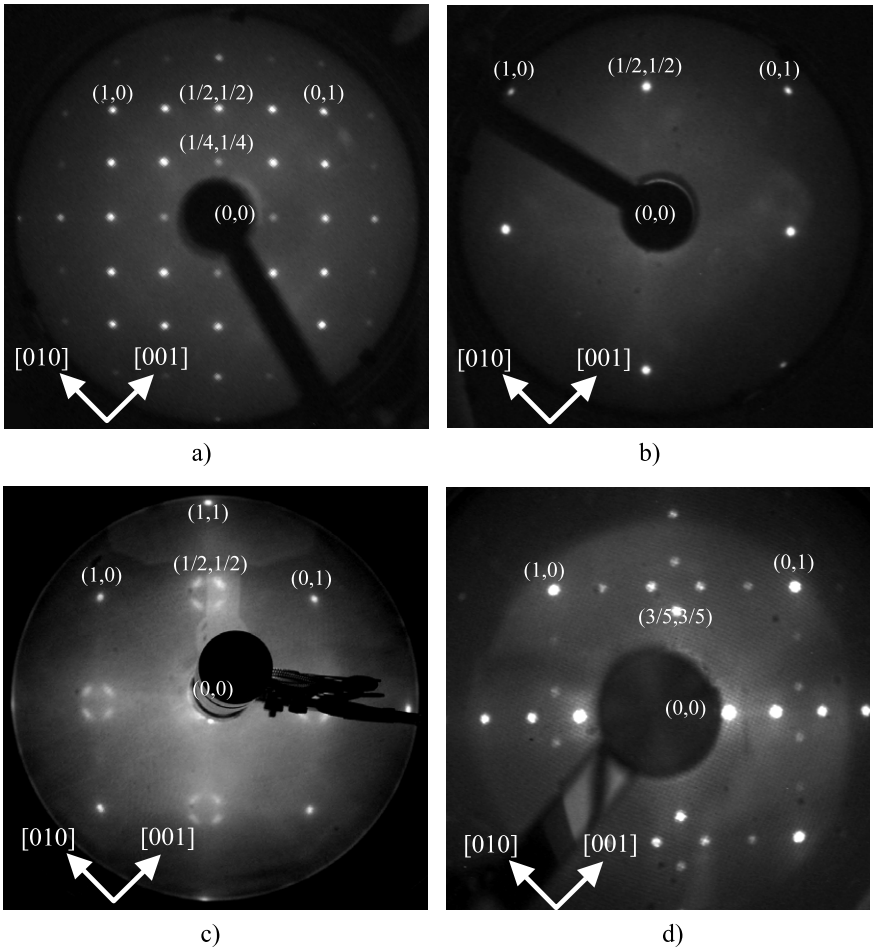

Figure 2. LEED patterns of the room temperature phases of the Pb/Cu(100) system for a coverage between 0 and 0.6 ML. The phase superstructure and the coverage are written at the bottom of the LEED images. The electron energy used was 70 eV. (a) c(4 × 4)-0.375 ML, (b) c(2 × 2)-0.5 ML, (c) split c(2 × 2) 0.53 ML, (d) c($5\sqrt{2} \times \sqrt{2}$)R45° 0.6 ML.

located at the APE beamline. The surface and bulk bands were mapped in a window of approximately 2 eV below the Fermi energy using a Scienta electron analyzer. In this chamber, the polarization plane of the light was horizontal and coincided with the measuring plane. The analyzer energy resolution was 20 meV and the angle resolution was 0.12°. When photoemission intensity is represented in a grey scale, white corresponds to high intensity. The Cu(100) sample was cleaned by Ar sputtering and annealing until a sharp (1 × 1) LEED pattern was observed. The quality of the surface was checked by measuring the narrow d-like surface state of odd symmetry at $\bar{\mathrm{M}}$. Pb was deposited from a Knudsen cell with the sample kept at room temperature. One ML is defined in this paper as the atomic density of the Cu(100) surface (1.54×10^{15} at cm^{-2}). The coverage is calibrated from the sequence of submonolayer structures and the evaporation time. As some of them appear alone in a narrow coverage range, this procedure gives an accuracy of at least 5%. Symmetry points are referred to the Cu(100) surface Brillouin zone. k_x corresponds to the $\overline{\Gamma\mathrm{M}}$ direction in this paper.

The LEED patterns of the room temperature phases of Pb/Cu(100) for coverages below 0.6 ML are shown in figure 2. Very precise deposition times of a well calibrated evaporator are necessary to obtain pure phases. Even if it is not the case for the phases that were measured, it is convenient to point out that Pb atoms sublimate from the surface at temperatures higher than 700 K, making it possible in this way to obtain a certain phase by evaporating slightly more Pb and then by sublimating the extra amounts by annealing for short periods of time at temperatures of around 700 K. We have identified in a previous paper [27] a phase transition for the c($5\sqrt{2} \times \sqrt{2}$)R45° structure at a coverage of 0.6 ML. When annealing the c($5\sqrt{2} \times \sqrt{2}$)R45° structure at a temperature of 450 K, a sharp transition takes place to a split the c(2 × 2) phase. The split c(2 × 2) phase shows the same LEED pattern as the one obtained with less Pb coverage at room temperature (a(5 × 5)R $\tan^{-1}(3/4)$ phase).

3. Results

3.1. Projected band gaps of the Cu(100) surface

Knowledge of the substrate electronic structure properties is a necessary condition in order to understand the interface electronic structure. In general, surface electronic states are localized in the projected band gap of the crystal. In the

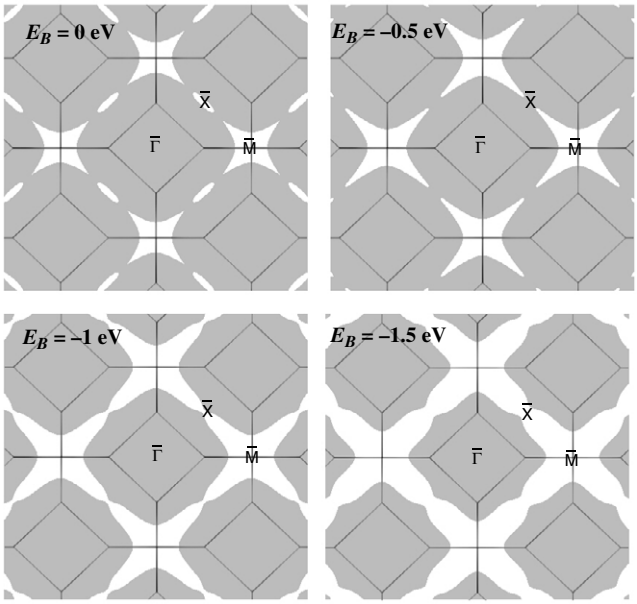

Figure 3. Projection of bulk bands of Cu (grey) along the [100] direction at constant binding energies. White areas correspond to absolute band gaps at each binding energy. The binding energy value is at the top left corner of each image.

case of Cu, it is a relatively simple task to obtain the $E(\mathbf{k})$ localization of the projected band gaps for a specific surface. The electronic structure of Cu has been successfully described theoretically [30]. A more than acceptable agreement between the theory and experiment exists [30], and parameters for a simplified tight binding model have been calculated [31]. In this section, the $E(\mathbf{k})$ localization of the projected band gaps of Cu(100) is shown. Calculations have been performed making use of a simple tight binding model [29]. Part of this information can be found in the literature [30], but it is useful to collect here a detailed view.

Figure 3 shows the momentum projected band gaps of Cu(001) for several constant binding energies. At the Fermi level (0 eV binding energy), a star-like gap is observed at the $\bar{\mathrm{M}}$ point and an ellipse-like smaller gap is observed at the $\bar{\mathrm{X}}$ point. The $\bar{\mathrm{M}}$ gap is increasing in size when the binding energy decreases, until the moment when a continuous gap joining $\bar{\mathrm{M}}$ and $\bar{\mathrm{X}}$ points is observed. At the $\bar{\mathrm{X}}$ point, the gap is closing for a binding energy of -0.5 eV, then the gap reopens for lower binding energies.

Figure 4 shows the projected band gaps along several radial $k_\parallel$ lines starting from $\overline{\Gamma\mathrm{M}}$ and ending along $\overline{\Gamma\mathrm{X}}$. Figure 4(a) shows the situation when $k_\parallel$ runs along the $\overline{\Gamma\mathrm{M}}$ direction. Between the Fermi level and -1.9 eV, a large gap is observed at the $\bar{\mathrm{M}}$ point. For the $\overline{\Gamma\mathrm{X}}$ direction, this gap becomes smaller and shifts completely to the occupied states. On the other hand, a gap observed in the unoccupied states in figure 4(c) for an angle of 10° off the $\overline{\Gamma\mathrm{M}}$ direction is approaching the Fermi level upon increasing the azimuthal angle. On the surface $\bar{\mathrm{X}}$ point, this gap is slightly entering the occupied states, as shown in figure 4(g).

3.2. Filling of a surface electronic band

We investigate in the following the surface electronic structure of Pb/Cu(100) as a function of Pb coverage below 0.7 ML. As Pb coverage increases, a growing number of electrons from the Pb overlayer have to be accommodated in occupied states of the forming structure. We will show that a result of the deposition of Pb atoms on the surface is the formation of allowed energy states in the Cu crystal band gaps, which change with Pb coverage.

Recent angle-resolved photoemission studies on In/Cu(100) [22] and Sn/Cu(100) [24] have focused on the Cu $\bar{\mathrm{M}}$ gap and have identified a surface state lying in this gap. This surface state has been assigned to have an adsorbate-substrate sp-like orbital origin [25, 26]. Figure 5 shows that a state of similar properties is observed for all Pb coverages in the sub-monolayer range in the Cu(100) $\bar{\mathrm{M}}$ gap. A surface state band with specific features is observed for each coverage. On the other hand, it was not possible in our apparatus to perform photoemission experiments while depositing Pb. For this reason, and in order to measure coverage-dependent changes in the most accurate way, the experiments in figure 5 were made using 50 eV photon energy. For this high photon energy value, both the Cu(100) substrate sp band and the surface state appear in the same Scienta $E(k)$ window. As the Fermi momentum of the bulk band does not depend on the coverage, this enables an accurate measurement of the surface state Fermi momentum, which is determined from the distance to the bulk band Fermi momentum. The accuracy degree is basically as high as the analyzer angular resolution. On the other hand the angular resolution for this high photon energy value is less than at lower photon energies, and features of the fine structure of the surface state can be lost, but the main purpose of the measurement can be achieved.

Figure 5 shows the effect of increasing the Pb coverage on the band dispersion along $\overline{\Gamma\mathrm{M}}$ direction. For 50 eV photon energy, the bulk sp band crosses the Fermi level at $k_\parallel = 1.35$ Å^{-1}. Emerging from the edge of the $\bar{\mathrm{M}}$ gap defined by the sp band, a new state is gradually shifting to the right as coverage increases. From figures 5(a) to (g), the Pb coverage increases from 0.3 to 0.7 ML. Figure 5(a) corresponds to 0.3 ML Pb coverage. As this coverage value is slightly less than the one required to obtain a c(4 × 4) structure, it is called an 'underdosed c(4 × 4)'. A close look at the data shown in figure 5(a) reveals that the sp band presents an extra shoulder, better contrasted for binding energies below -1 eV. Figure 5(b) corresponds to a c(4×4) surface structure, obtained for 0.375 ML. The band dispersion shows now the shoulder out of the sp band, but still very close to it. For the c(2 × 2) surface structure at 0.5 ML Pb coverage, figure 5(c) shows the surface state shifted to higher $k_\parallel$ values compared with lower coverages. This behaviour continues as coverage increases, as shown in figures 5(d)–(g), where the dispersions corresponding to (d) 0.52, (e) 0.55, (f) 0.6 and (g) 0.7 ML of Pb are plotted. For the precise Pb coverages corresponding to the c(4 × 4) phase and the c($5\sqrt{2} \times \sqrt{2}$)R45° phase, extra features besides the analysed surface state are observed. Resolving these features requires the use of lower photon energy values, where

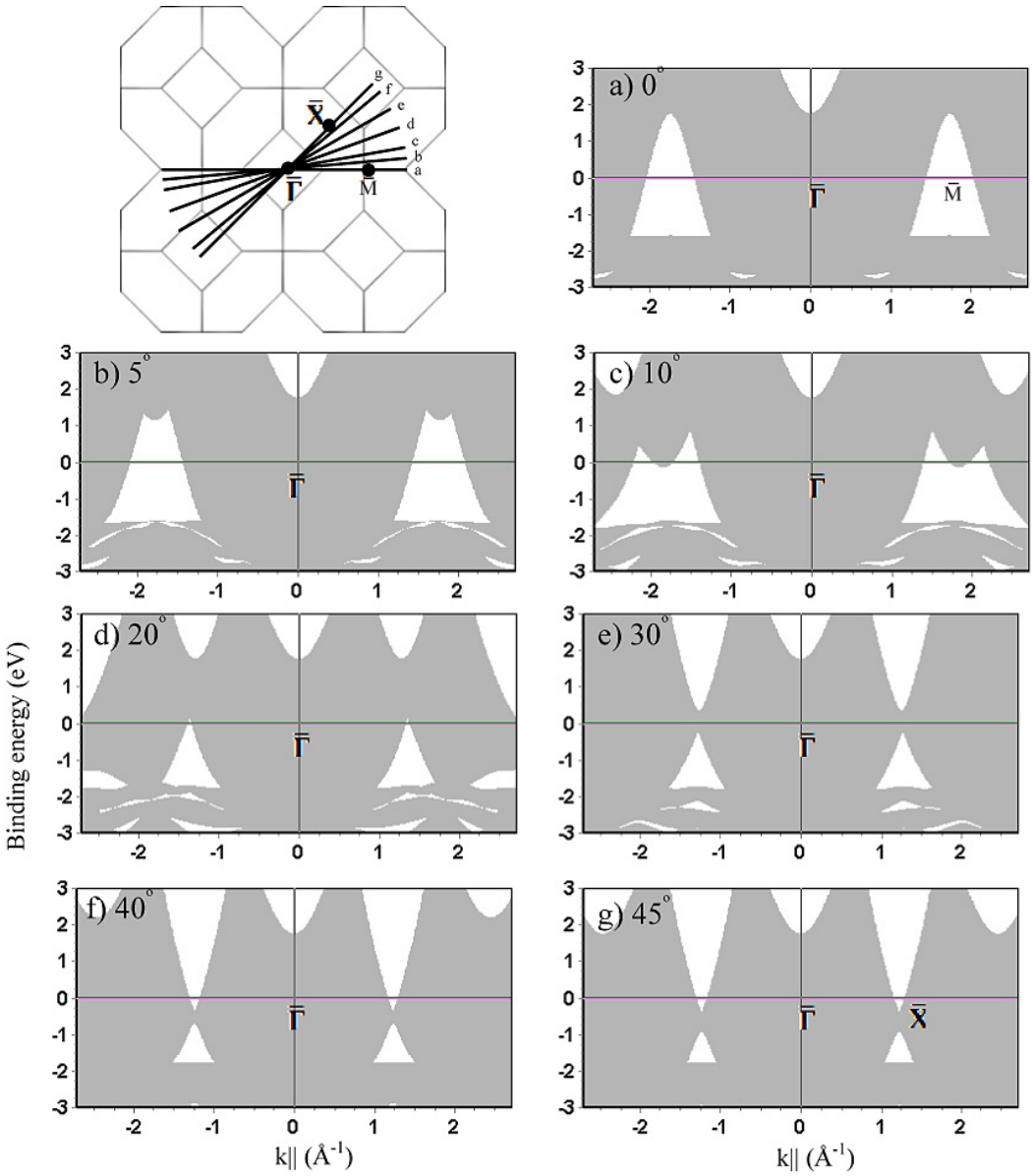

Figure 4. Projected band gap structure along radial $k_\parallel$ lines starting from $\overline{\Gamma M}$ (a) and going to $\overline{\Gamma X}$. The left top image shows the momentum position of the $k_\parallel$ lines where the band projection has been calculated. The angle displayed in the images from (a) to (g) represent the azimuthal off-angle with respect to the $\overline{\Gamma M}$ direction.

the angular dispersion of the state gives better $k_\parallel$ precision. This topic is discussed in section 3.3 for the c(4 × 4) phase and in [27] for the c($5\sqrt{2} \times \sqrt{2}$)R45° phase.

Figure 6 shows a series of selected momentum distribution curves (MDCs) obtained from figure 5. The Pb induced surface state appears as a shoulder shifting with coverage to higher parallel momentum values. As the shape of the surface band remains unchanged, the shift of the crossing point (Fermi momentum) represents an increased filling of the band (compare with the quasi-circular Fermi surfaces observed in the case of Sn/Cu(100) in [28] and figure 13). An illustrative interpretation of this band filling situation is given in figure 7. A free-electron-like parabolic dispersion has been fitted to the experimental dispersion of the surface state shown in figure 7, i.e. $E(k_\parallel) = Ak_\parallel^2 + B$, where A and B are parameters obtained from the fit. The data used for fitting the theoretical parabola are given by the dispersion of the surface state in the $\bar{\text{M}}$ gap region (data shown in figure 5 and highlighted with bold lines in figure 7). For the lowest coverage of 0.3 ML, no points could be extracted due to the difficulty of locating the state on the sp band shoulder. The parameters obtained from the fit are given in table 1. For the c(4 × 4) phase, the errors in the fitting are larger because the surface state is quite close to the bulk sp band. The values from table 1 show a gradual increasing in the band filling. The parameter A, corresponding to the curvature of the parabola, is approximately constant within experimental accuracy, while B decreases continuously with coverage. The picture deduced from this observation is that the parabolic band becomes deeper, keeping a constant shape, i.e. the band is progressively filled as coverage increases.

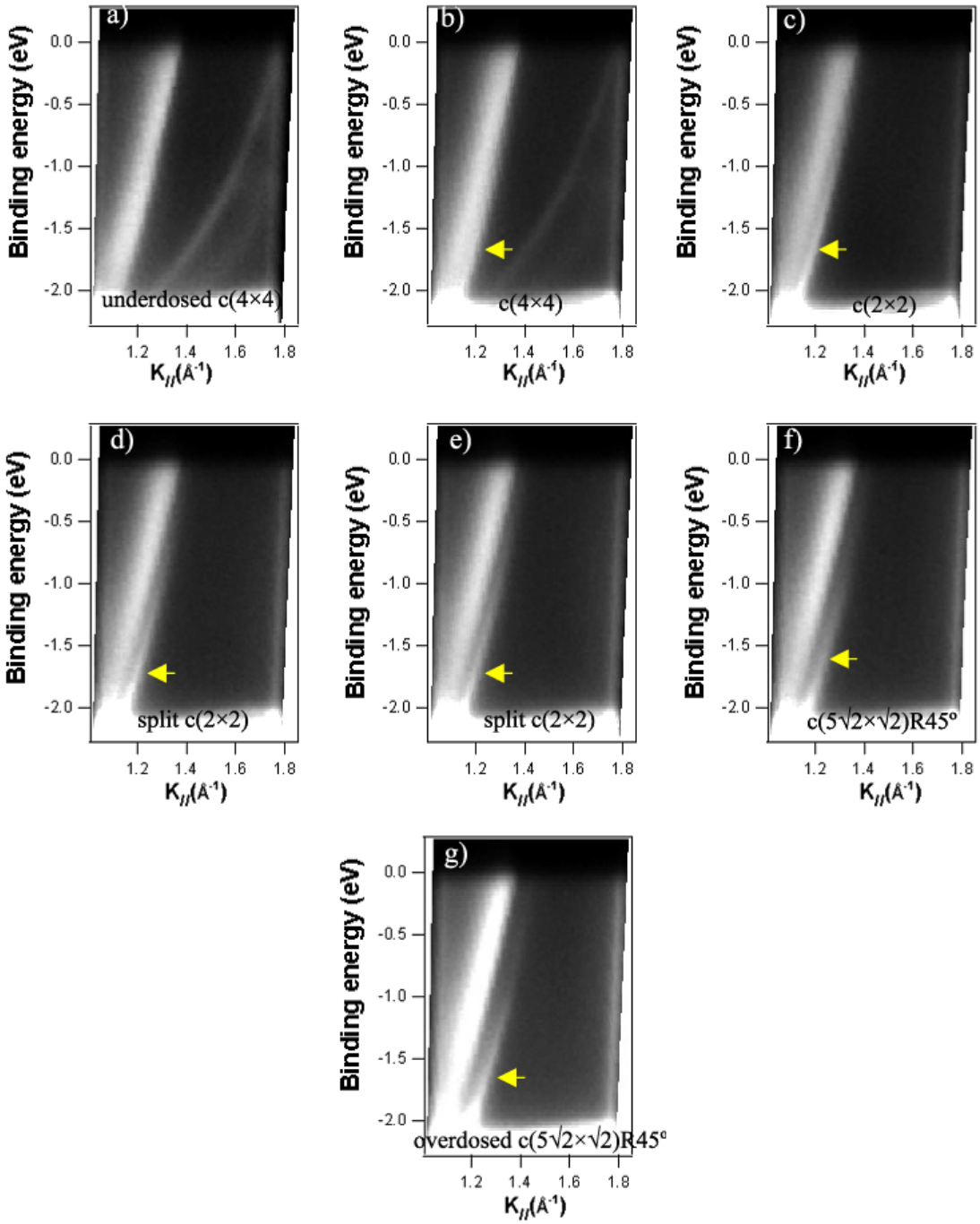

Figure 5. Sequence of valence band scans (binding energy versus parallel momentum in grey scale) for Pb/Cu(100) along the $\overline{\Gamma M}$ direction measured for 50 eV photon energy. The scans correspond to an increasing Pb coverage, starting for 0.3 ML (a) and ending with an overdosed c($5\sqrt{2} \times \sqrt{2}$)R45° phase at 0.7 ML (g). The broad band at low $k_{\|}$ values crossing the Fermi level at 1.35 Å^{-1} is the bulk copper sp band. The yellow arrow indicates a surface state. (b) $\Theta = 0.375$ ML, (c) 0.5 ML, (d) 0.52 ML, (e) 0.55 ML, (f) 0.6 ML, (g) 0.7 ML.

The band filling has been estimated assuming a quasi-circular contour at the Fermi level, with different values of the Fermi momentum along $\overline{\Gamma M}$ and $\overline{\Gamma X}$ (see also section 3.3 and figure 13, which shows one contour for the c(4 × 4) phase). The band filling is twice the result of dividing the area enclosed by the contour by the area of the (1 × 1) unit cell (where a band filling of 2 corresponds to a completely filled band). The Fermi momentum along $\overline{\Gamma M}$ is obtained from the fit made in figure 6, the value along $\overline{\Gamma X}$ is obtained from Fermi contours.

This analysis of the behaviour of the surface state observed for increasing coverages shown in figures 5 and 6, demonstrates that the shift of the surface state is gradual, indicating that the physical phenomenon corresponds to an increasing filling of the surface state band. This effect has been observed in several metal/semiconductor interfaces, where

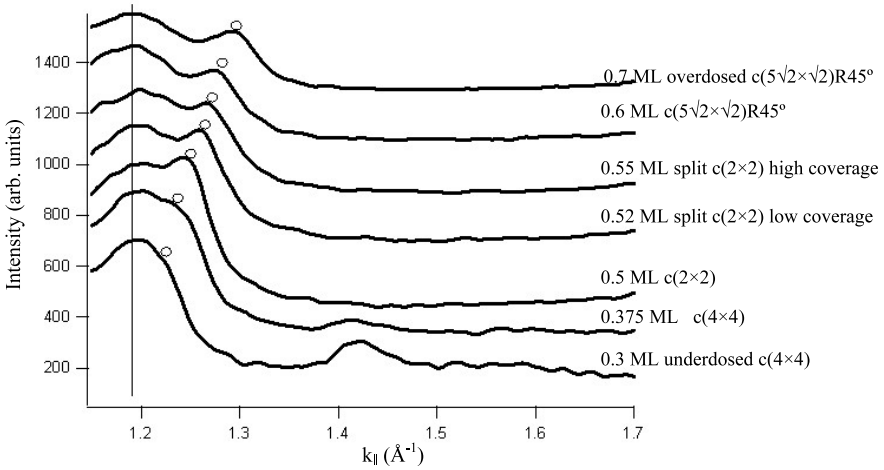

Figure 6. Momentum distribution curves at $E_B = -1.7$ eV from the scans shown in figure 5. The bottom profile corresponds to the lowest Pb coverage of 0.3 ML. The circle on top of the surface state peak shows the shift of the state with increasing Pb coverage.

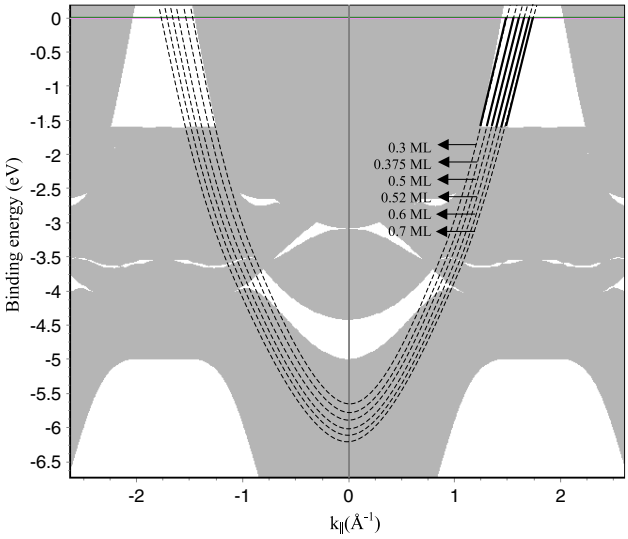

Figure 7. Illustration of the surface band filling with increasing Pb coverage for the Pb/Cu(100) interface. Dotted lines correspond to a parabolic dispersion along the $\overline{\Gamma}\overline{M}$ direction of a free-electron-like surface state band. Portions of this parabola represented with a bold black line within the $\bar{M}$ gap correspond to the observed surface state.

the amount of filling of the surface bands depends on the coverage [33]. No such effect is expected for the deposition of a metal on top of another metal, due to the insignificant contribution of surface electrons to the density of states at the Fermi energy with respect to the bulk contribution. The case of Sn/Cu(100) has been recently analysed using the density functional theory [32]. The results support the fact that the surface band is traced back to the formation of a surface alloy, i.e. to substrate mediated interactions between the adsorbates. Using this image for the Pb/Cu(100) case, which is very close to Sn/Cu(100) in many properties, the progressive band filling observed could be attributed to an enhanced interaction between adsorbate atoms due to the decrease in their mean interatomic distance for increasing coverages.

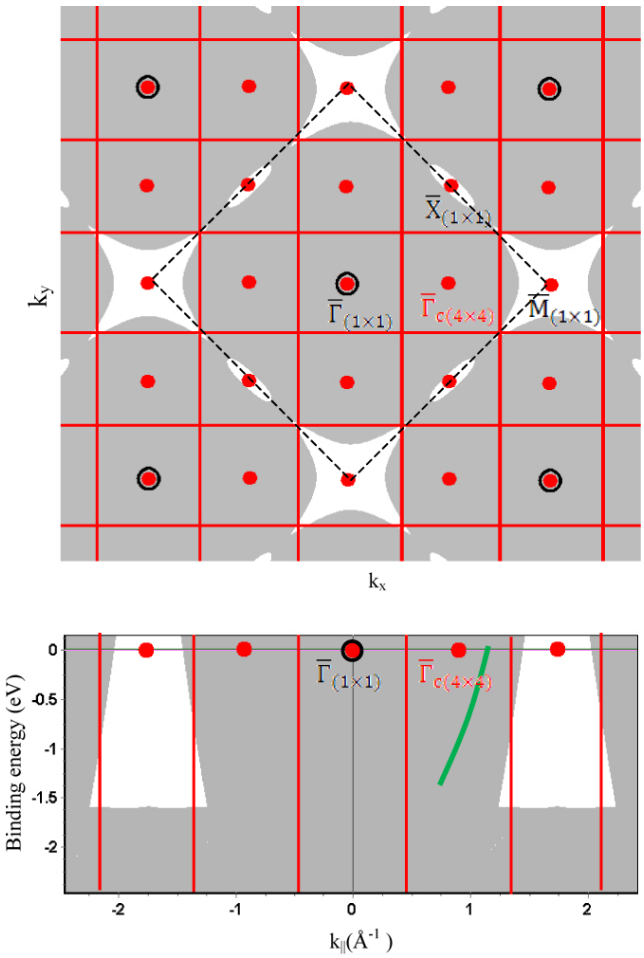

Figure 8. Top: surface Brillouin zones of the c(4 × 4) structure. The $\bar{\Gamma}$ points of the c(4 × 4) phase are marked with red (gray) dots, while red (gray) lines mark the zone edges. The $\overline{\Gamma}$ (black circles), $\bar{M}$ and $\bar{X}$ symmetry points of the unreconstructed (1 × 1) surface are also plotted. The dotted line corresponds to the (1 × 1) Brillouin zone boundary. The grey shadowed area corresponds to the band bulk projection at the Fermi level, while white areas correspond to absolute band gaps. Bottom: band gap along $\overline{\Gamma}\overline{M}$ together with the symmetry points of the c(4 × 4) structure. The green (gray) line shows the theoretical position of the Cu sp band when probed with 27 eV photons.

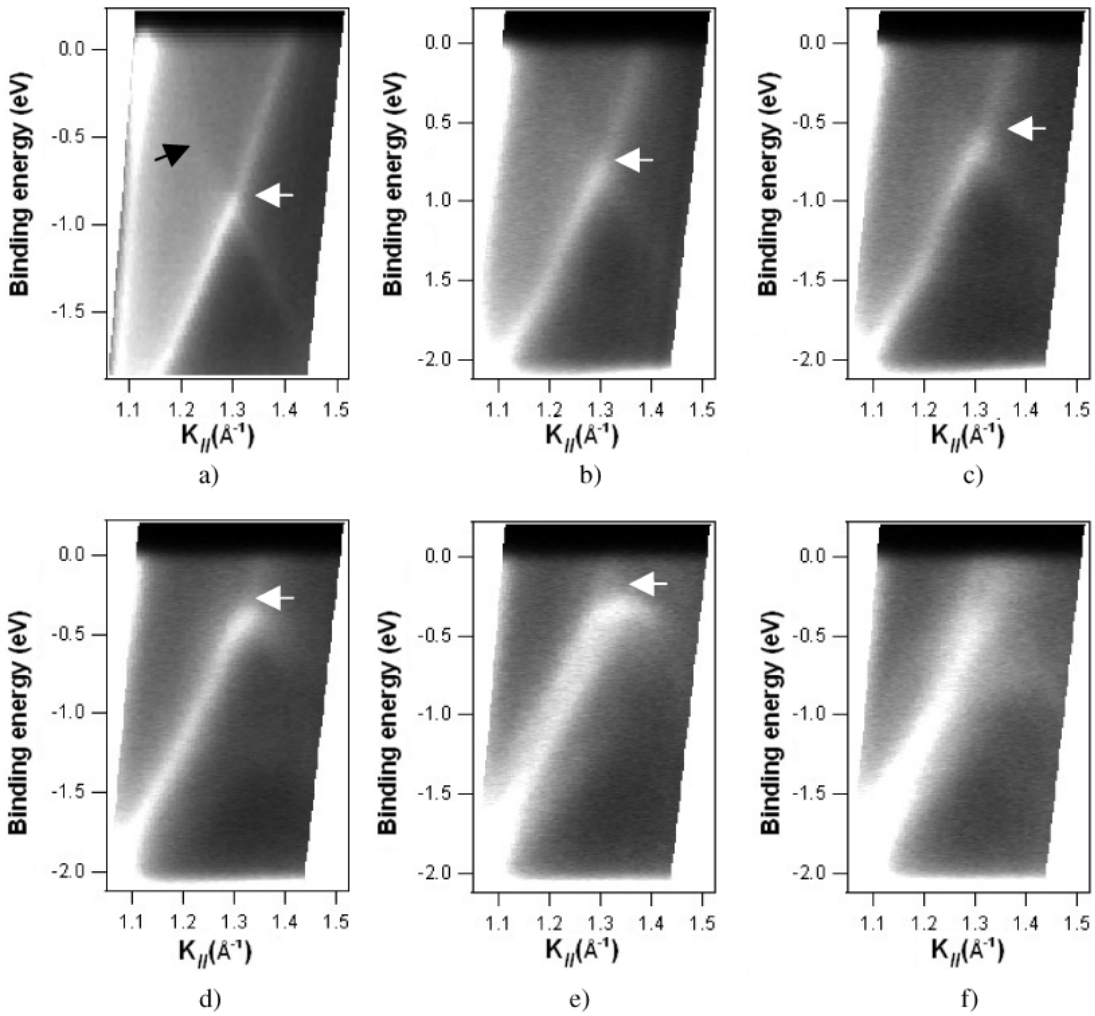

Figure 9. Sequence of valence band scans (binding energy versus parallel momentum in grey scale) for Pb/Cu(100)-c(4 × 4) along different azimuthal directions measured with 27 eV photons. The first image (a) corresponds to the $\overline{\Gamma M}$ direction (0°), and the subsequent images to azimuthal angles of (b) 4°, (c) 8°, (d) 12°, (e) 16°, (f) 20° off the $\overline{\Gamma M}$ direction.

Table 1. Parameters from a parabolic fit to the data of figure 7.

Phase	Coverage (ML)	A (eV Å^{-2})	B (eV)	Band filling
c(4 × 4)	0.30	2.85 ± 0.20	-5.75 ± 0.2	1.41 ± 0.02
c(2 × 2)	0.375	3.03 ± 0.03	-6.01 ± 0.1	1.47 ± 0.01
Split c(2 × 2)	0.50	2.97 ± 0.07	-6.04 ± 0.02	1.48 ± 0.01
Split c(2 × 2)	0.52	3.07 ± 0.06	-6.18 ± 0.02	1.52 ± 0.01
c($5\sqrt{2} \times \sqrt{2}$)$R45°$	0.60	3.02 ± 0.02	-6.26 ± 0.02	1.54 ± 0.01
c($5\sqrt{2} \times \sqrt{2}$)$R45°$	0.70	2.89 ± 0.05	-6.30 ± 0.02	1.55 ± 0.01

3.3. Electronic structure of the c(4 × 4) phase

The c(4 × 4) phase is obtained for a precise coverage of 0.375 ML of Pb. A thorough experimental procedure making use of a well calibrated Pb evaporator is required to achieve a uniform coverage of 0.375 ML. The top panel of figure 8 shows the surface Brillouin zones of the c(4 × 4) structure. Red circles correspond to the $\bar{\Gamma}$ points of the c(4 × 4) phase and red lines to the zone boundaries of the same structure. The zone boundary of the unreconstructed (1 × 1) substrate is drawn with a dotted black line. The symmetry points of the unreconstructed (1 × 1) surface $\bar{\Gamma}$, $\bar{\mathrm{M}}$ and $\bar{\mathrm{X}}$ are also shown. The grey shadowed area of figure 8 is the bulk band projection of Cu along the [100] direction at the Fermi level. The projection has been included as guidance to the regions of interest from the electronic structure point of view.

The bottom panel of figure 8 shows the symmetry lines of the c(4 × 4) structure along the $\overline{\Gamma M}$ direction in a binding energy versus $k_{\parallel}$ plot. The bulk Cu sp band projection shows the position of the projected band gap along the [100] direction with respect to the c(4 × 4) symmetry lines for the $\overline{\Gamma M}$ direction. At the Fermi level, the c(4 × 4) zone edge is out

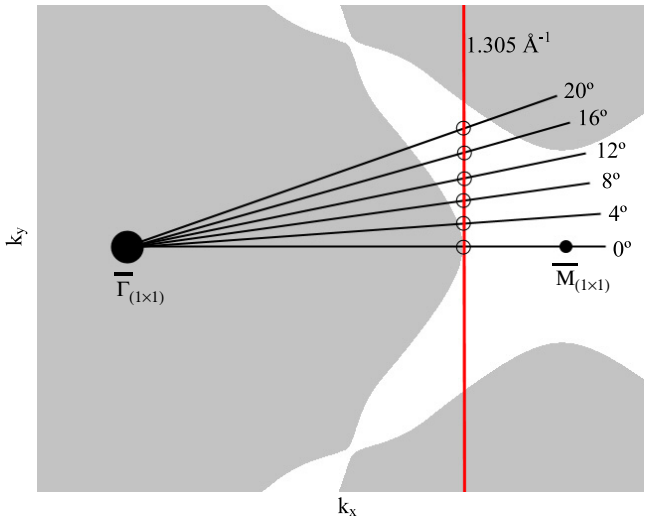

Figure 10. Reciprocal space map showing the location of the backfolding points for the surface state band. The folding points are shown as black empty circles and follow the zone boundary of the c(4 × 4) structure (red line). The Cu band projection (grey shaded region) has been calculated for a binding energy of −0.95 eV in order to highlight the fact that the folded state lies in a bulk band gap all the time.

of the $\bar{M}$ gap. Between binding energies of −0.7 and −1.6 eV, the zone edge of the c(4 × 4) structure is within the $\bar{M}$ gap.

Angle-resolved photoemission measurements have been performed using a photon energy of 27 eV. More angular resolution is achieved than using 50 eV, and the bulk band of Cu stays away from the $\bar{M}$ gap. leaving a larger region without bulk states for this photon energy. The Cu sp band for 27 eV is shown with a green line in the bottom panel of figure 8. The band has been calculated using a tight binding approximation [29].

Figure 9(a) shows the binding energy versus $k_\parallel$ measurement along the $\overline{\Gamma M}$ direction. The subsequent images are analogous scans for different azimuthal angles off $\overline{\Gamma M}$: (b) 4°, (c) 8°, (d) 12°, (e) 16°, (f) 20°. The bright band crossing the Fermi level at $k_\parallel = 1.15$ Å^{-1} in figure 9(a) is the Cu sp bulk band.

Two other states are observed in figure 9. The first one is the surface state band already discussed in section 3.2. It shows parabolic dispersion, stays close to the edge of the $\bar{M}$ gap and it crosses the Fermi level at $k_\parallel = 1.4$ Å^{-1}. A weaker second band marked with a black arrow is also observed. It looks like a band backfolded from the surface state with respect to the zone boundary (1.305 Å^{-1}). The folding point is marked with a white arrow in figure 9. As shown in figure 10, the $k_\parallel$ position of the folding points corresponds always to the zone boundary edge of the c(4 × 4) structure.

Two states were also observed in the $\bar{M}$ gap for Sn/Cu(100)-(3$\sqrt{2}$ × $\sqrt{2}$)R45° [24, 28]. The second state was explained by the two-domain nature of the structure. The c(4 × 4) structure is a single domain structure and an explanation based on the existence of multiple domains cannot be valid. In the following we provide the clues for explaining the origin of this state. The band dispersion from figure 11 shows two bands folded with c(4 × 4) symmetry, exposing an avoided crossing band gap in the occupied states (see also figure 9, white arrows). The binding energy value of the band gap approaches the Fermi level as the azimuthal angle off the $\overline{\Gamma M}$ direction increases. For an azimuthal angle of 16° off the $\overline{\Gamma M}$ direction, the gap is at the Fermi level (figure 9(e)), while for larger angles the gap will appear in the empty states. A gap at the Fermi level of a state that has mostly a free electron character is producing an overall decrease in the total electronic energy of the structure and therefore it contributes to the stabilization of the structure. The extent and relevance of this effect cannot be determined from the

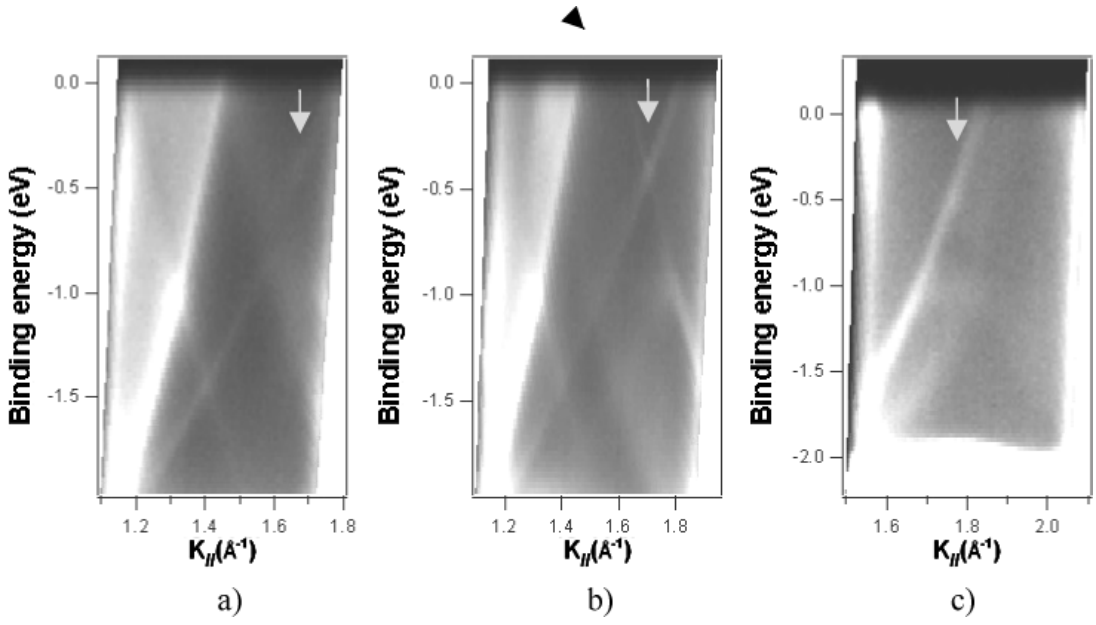

Figure 11. Band dispersion along the $\overline{\Gamma M}$ direction for Pb/Cu(001)-c(4 × 4) measured at $h\nu = 32$ eV (a), 37 eV (b) and 50 eV (c).

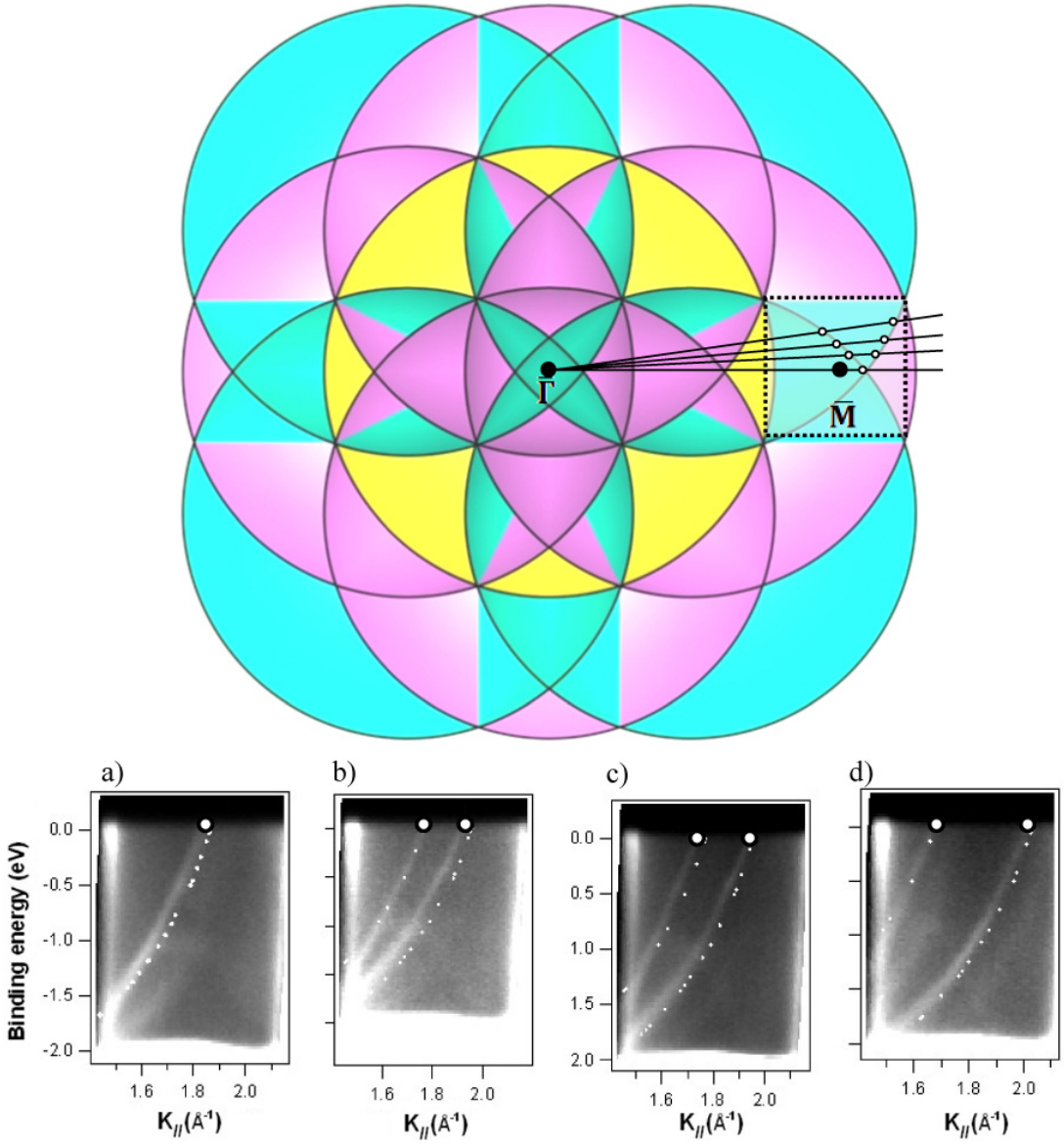

Figure 12. Top: free-electron-like paraboloids identical to the original surface state band are replicated centred at {1/4, 1/4} symmetry points in order to reflect the c(4 × 4) symmetry. Dashed lines show one c(4 × 4) Brillouin zone in the $\bar{M}$ point area, which is the range probed in the experiment (bottom panel). For simplicity, only the c(4 × 4) Brillouin zone around the $\bar{\Gamma}$ point shows the full c(4 × 4) folding. Bottom: band dispersion at 50 eV photon energy for the c(4 × 4) Pb/Cu(001) phase: (a) along the $\overline{\Gamma M}$ direction, and for $k_{\|}$ directions off the $\overline{\Gamma M}$ direction by (b) 1.5°, (c) 3° and (d) 4.5°. The white dots superimposed on the experimental data correspond to the intersection of the semiempirical free-electron-like paraboloids centred at {1/4, 1/4} symmetry points, as shown in the top panel. Note the good agreement between the experimental bands and the prediction from the folded paraboloids.

data shown here, and a more detailed investigation studying the temperature dependence of the gap would be required. However, it is interesting to recall that a similar Fermi level band gap has been observed for In/Cu(100)-c(4 × 4) [23], where its existence was correlated with the superstructure stability.

Figure 11 shows high-resolution valence band images along the $\overline{\Gamma M}$ direction taken for three photon energies: 32 eV (a), 37 eV (b) and 50 eV (c). These images reveal the presence of additional electronic states in the $\bar{M}$ gap region of the c(4 × 4) phase, which seem to reflect multiple folding and several avoided crossing band gaps (e.g. for $k_{\|} \cong 1.4$ Å^{-1} and a binding energy of −1.5 eV, best seen at 32 eV photon energy; for $k_{\|} \cong 1.7$ Å^{-1} and a −0.4 eV binding energy, best seen at 37 eV photon energy, etc).

The state marked with a white arrow in figure 11 is observed at $k_{\|}$ values around 1.6 Å^{-1} for all the three photon energies used. The crossing of the Fermi level is at $k_{\|} = 1.79$ Å^{-1} (the most precise determination of this value is made for 50 eV photon energy). This behaviour (constant $k_{\|}$ for different photon energies) indicates a surface origin of the state. A straightforward explanation for the multiple states seen in figure 11 is a c(4 × 4) folding of the surface band, i.e. the quasi-circular surface band observed for a broad coverage range in figure 5 is folded with the full c(4 × 4) symmetry to reflect the surface periodicity for this coverage.

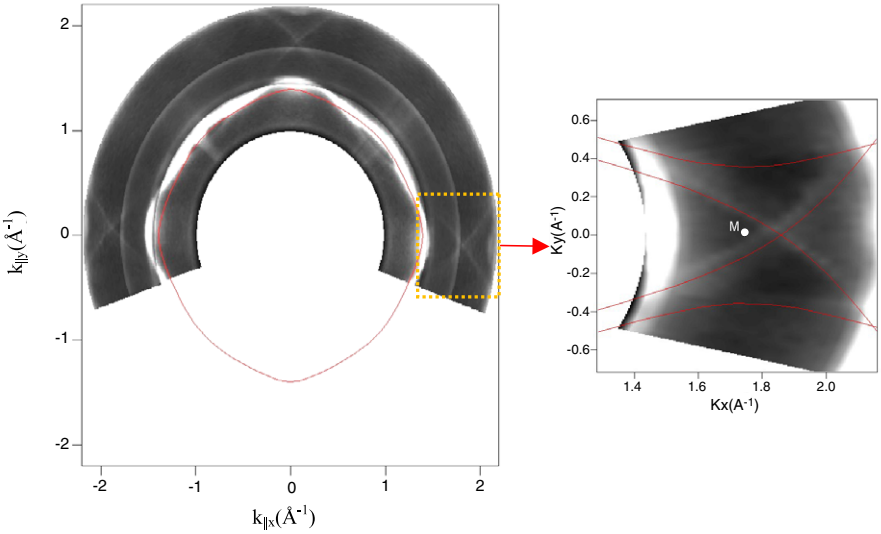

Figure 13. Left: Fermi surface slice for Pb/Cu(100)-c(4 × 4) at a photon energy of 50 eV. The red line is the theoretical calculation for the sp band position at 50 eV. The dashed rectangle in yellow is shown in the right panel. Right: an enlargement around the $\bar{M}$ point of the Fermi surface. Red lines correspond to the c(4 × 4) folding of the surface state.

We show in the following, several pieces of experimental evidence supporting this explanation, in particular a detailed two-dimensional mapping at 50 eV photon energy has been performed.

In order to understand the origin of the extra states observed, we construct first a semiempirical free-electron-like state with the shape of a paraboloid. For simplicity, and taking into account that the experimental data are taken around the $\bar{M}$ point band gap, we construct a rotation paraboloid (i.e. the Fermi contour is a circle). The parabola parameters are taken from table 1 for 0.375 ML Pb coverage (c(4 × 4) phase). Next, the paraboloid is folded with the c(4 × 4) structure periodicity (figure 12, top). The bottom panel of figure 12 shows azimuthal scans taken at 50 eV photon energy and for small angles off the $\overline{\Gamma M}$ direction. Panel (a) of figure 12 (bottom) shows the band dispersion at 50 eV along the $\overline{\Gamma M}$ direction for the Pb/Cu(100)-c(4 × 4) phase. The other three plots in the panel correspond to $k_{\parallel}$ directions off the $\overline{\Gamma M}$ direction by 1.5° (b), 3° (c) and 4.5° (d). Along the $\overline{\Gamma M}$ direction, a single state is observed crossing the Fermi level at $k_{\parallel} = 1.79$ Å^{-1}. The origin of this state is traced back to the intersection of the surface band centred at $\{1/4, 1/4\}$ symmetry points. For an azimuthal angle off $\overline{\Gamma M}$ of only 1.5°, the band dispersion reveals two split bands (figure 12(b)). The amount of the splitting increases very fast with the azimuthal angle, as shown in figures 12(c) and (d), which show the band dispersion along $k_{\parallel}$ directions 3° and 4.5° off the $\overline{\Gamma M}$ direction. All the states observed are easily explained by performing the intersections of the paraboloids mentioned before. The white dots in the bottom panels of figure 12 correspond to the semiempirical free-electron-like paraboloids centred at $\{1/4, 1/4\}$ symmetry points shown in the top panel of figure 12. It is interesting to note that the most intense folding corresponds indeed with $\{1/4, 1/4\}$ points.

Figure 13 shows a slice of the Fermi surface for the c(4 × 4) phase taken at 50 eV photon energy. At this photon energy the bulk Cu sp band is very close to the gap edge, as shown by the red line contour, which is the theoretical prediction of the sp band position from the tight binding model at a spherical cut corresponding to a photon energy of 50 eV. Due to this reason, the strong quasi-circular contour observed in figure 13 corresponds to both the bulk sp band and the surface state band, which appear very close in reciprocal space at this photon energy. The right side of figure 13 shows an enlargement of a window centred at the $\bar{M}$ point, where red lines correspond to a c(4 × 4) folding of the surface state. Note that data at 50 eV alone could not distinguish between a c(4×4) folding of the surface state or a c(4×4) Umklapp of the Cu bulk sp band, as both are hard to distinguish at this photon energy. However, the data taken at other photon energies reveal that the surface folding is the only acceptable explanation.

4. Conclusions

From both structural and electronic structure points of view, the Pb/Cu(001) system shows a rich variety of phenomena. A novel gradual filling of an electronic surface state with increasing Pb coverage has been observed when measuring the surface state dispersion along the $\overline{\Gamma M}$ direction. Folding of this state is observed in the occupied states for the c($5\sqrt{2} \times \sqrt{2}$)R45° (reported in [27]) and c(4 × 4) structures at their corresponding symmetry points. The electronic states of the c(4 × 4) structure can be understood considering a nearly free-electron-like behaviour of the surface state observed in the $\bar{M}$ gap and folding of this state with the c(4 × 4) periodicity. The electronic structure contribution to the stabilization of the c(4 × 4) Pb/Cu(001) phase has been analysed. Portions of the c(4×4) reciprocal space out of high symmetry directions show a surface state folded and exposing the gap at the Fermi level, suggesting an electronic contribution to the phase stability.

Acknowledgments

Financial support by the Spanish MICINN (FIS2008-00399) and by CAM (S-0505/PPQ/0316) is gratefully acknowledged.

Work at Elettra is supported by the EU under contract No. RII3-CT-2004-506008 (IA-SFS).

References

[1] Bauer E, Schommers V and von Blanckenhagen P 1987 *Structure and Dynamics of Surfaces II* (Berlin: Springer)
[2] Mascaraque A and Michel E G 2002 *J. Phys.: Condens. Matter* **14** 6005
[3] Persson B N J 1992 *Surf. Sci. Rep.* **15** 1
[4] Tosatti E, Bertel E and Donath M 1995 *Electronic Surface and Interface States on Metallic Systems* (Singapore: World Scientific)
[5] Yeom H W, Takeda S, Rotenberg E, Matsuda I, Horikoshi K, Schaefer J, Lee C M, Kevan S D, Ohta T, Nagao T and Hasegawa S 1999 *Phys. Rev. Lett.* **82** 4898
[6] Swamy K, Menzel A, Beer R and Bertel E 2001 *Phys. Rev. Lett.* **86** 1299
[7] Schiller F, Cordon J, Vyalikh D, Rubio A and Ortega J E 2005 *Phys. Rev. Lett.* **94** 016103
[8] Gruner G 1994 *Density Waves in Solids* (Reading, MA: Addison-Wesley)
[9] Henrion J and Rhead G E 1972 *Surf. Sci.* **29** 20
[10] Hoesler W and Moritz W 1982 *Surf. Sci.* **117** 196
[11] Hosler W, Moritz W, Tamura E and Feder R 1986 *Surf. Sci.* **171** 55
[12] Hosler W and Moritz W 1986 *Surf. Sci.* **175** 63
[13] Sánchez A and Ferrer S 1989 *Phys. Rev.* B **39** 5778
[14] Li W, Lin J-S, Karimi M and Vidali G 1991 *J. Vac. Sci. Technol.* A **9** 1707
[15] Camarero J, Spendeler L, Schmidt G, Heinz K, de Miguel J J and Miranda R 1994 *Phys. Rev. Lett.* **73** 2448
[16] Robert S, Cohen C, L'Hoir A and Moulin J 1996 *Surf. Sci.* **365** 285
[17] Nagl C, Platzgummer E, Haller O, Schmid M and Varga P 1995 *Surf. Sci.* **331–333** 831
[18] Robert S, Gauthier S, Bocquet F and Rousset S 1996 *Surf. Sci.* **350** 136
[19] Plass R and Kellogg G L 2000 *Surf. Sci.* **470** 106
[20] Kellogg G L and Plass R 2000 *Surf. Rev. Lett.* **7** 649
[21] Nakagawa T, Boishin G I, Fujioka H, Yeom H W, Matsuda I, Takagi N, Nishijima M and Aruga T 2001 *Phys. Rev. Lett.* **86** 854
[22] Nakagawa T, Mitsushima S, Okuyama H, Nishijima M and Aruga T 2002 *Phys. Rev.* B **66** 085402
[23] Nakagawa T, Okuyama H, Nishijima M, Aruga T, Yeom H W, Rotenberg E, Krenzer B and Kevan S D 2003 *Phys. Rev.* B **67** 241401
[24] Martinez-Blanco J, Joco V, Ascolani H, Tejeda A, Quiros C, Panaccione G, Balasubramanian T, Segovia P and Michel E G 2005 *Phys. Rev.* B **72** 041401
[25] Aruga T 2006 *Surf. Sci. Rep.* **61** 283
[26] Xing G, Yu-mei Zh, Si-cheng W and Ding-sheng W 2002 *Phys. Rev.* B **66** 073405
[27] Joco V, Martinez-Blanco J, Segovia P, Balasubramanian T and Michel E G 2006 *Surf. Sci.* **600** 3851
[28] Martínez-Blanco J, Joco V, Fujii J, Segovia P and Michel E G 2008 *Phys. Rev.* B **77** 195418
[29] Joco V, Mikuszeit N, Martinez-Blanco J and Michel E G 2009 at press
[30] Burdick G A 1963 *Phys. Rev.* **129** 138
[31] Papaconstantopoulos D A 1986 *Handbook of the Band Structure of Elemental Solids* (Berlin: Springer)
[32] Altmann K N, Crain J N, Kirakosian A, Lin J-L, Petrovykh D Y, Himpsel F J and Losio R 2001 *Phys. Rev.* B **64** 035406
[33] Fuhr J D, Gayone J E, Martınez-Blanco J, Michel E G and Ascolani H 2009 *Phys. Rev.* B submitted